Proceedings of DETC'03
ASME 2003 Design Engineering Technical Conferences and
Computers and Information in Engineering Conference
Chicago, Illinois, USA, September 2-6, 2003

DETC2003/PTG-48067

Mesh Phasing Relationships in Planetary and Epicyclic Gears

R. G. Parker
Department of Mechanical Engineering
Ohio State University
206 W. 18th Ave.
Columbus, OH 43210-1107
parker.242@osu.edu

J. Lin
John Deere Corporation
P. O. Box 8000
Waterloo, IA 50704-8000
linjacobj@waterloo.deere.com

Introduction

Planetary and epicyclic gears (Figure 1) rely on symmetry to achieve the large torque-weight ratios and compactness that make them widely used in multiple applications. A desirable design objective is to divide the load equally such that the multiple sun-planet tooth meshes carry nearly equal load with the same load equality for the ring-planet tooth meshes. To achieve this, one seeks to have all sun-planet meshes be *in-phase*, that is, each sun-planet mesh nominally has identical mesh conditions (*i.e.*, number of teeth in contact) at all times with similar conditions for the ring-planet meshes. Past research has shown, however, that differing mesh phasing between the sun-planet (and consequently ring-planet) meshes has powerful impact on the dynamic response and can have significant benefits in reducing vibration and noise [1-4]. In essence, designers have a variety of options and objectives in choosing the mesh phasing for a given application, and a clear understanding of the relations governing the mesh phasing is essential.

A lumped-parameter representation of a three-planet planetary (epicyclic) gear is shown in Figure 1. This is a typical model used in static and dynamic analyses. The springs between the sun-planet and ring-planet represent the meshing gear teeth. The stiffness of these meshes varies as the gears rotate because of the changing numbers of teeth in contact. In using these models for static or dynamic analyses, it is essential to correctly define the relative phase of these multiple tooth meshes as the gears rotate.

Despite a variety of papers [5-11] that deal with planetary gear dynamics and include mesh phasing in the models, there is inconsistency between these works that suggests confusion in the true mesh phasing. These models typically involve a variation of the basic schematic in Figure 1. Some of these models are in error in the treatment of phasing while others are conceptually correct but do not lay out the mathematical relations for mesh phasing. Private discussions with planetary gear researchers also suggest a general confusion on the details relating the following three quantities at the heart of this issue: phasing between the various sun-planet meshes, phasing between the various ring-planet meshes, and phasing between the ring-planet and sun-planet meshes at a given planet. This Technical Brief attempts to clarify the mesh phasing properties for general planetary (epicyclic) gears and provide a complete analytical description in terms of the fundamental parameters of tooth numbers and planet locations.

The journal version of this work will appear in [12].

Planet Mesh Phasing

The phase relationships in this work are defined in terms of *mesh tooth variation* functions $k_{sn}(t), k_{rn}(t)$ that represent the number of teeth in contact at the *n*th sun-planet and ring-planet meshes. These mesh tooth variation functions, which are *approximately* proportional to mesh stiffness variation, are time-dependent functions that are periodic over one mesh cycle. Because the mesh frequencies ω_m of the sun-planet and ring-planet meshes are equal, mesh tooth variations at the sun-planet and ring-planet meshes have equal periodicity $T_m = 2\pi/\omega_m$. While each of the sun-planet meshes has the same shape of mesh tooth variation, they are not in phase with each other. In other words, there is typically a time shift between the number of teeth in contact at two different meshes. Similar comments apply to the ring-planet meshes.

There is no attempt in this paper to examine any properties of the mesh stiffness variation (or closely related static transmission error) functions outside of their relative phasing. The shape of these functions depends greatly on the tooth modification, load, tooth geometry, *etc.*, and must be calculated with analyti-

cal or computational models. But, whatever the mesh stiffness variation shape for one sun-planet (ring-planet) mesh, other sun-planet (ring-planet) meshes will have the same shape with the exception of a possible phase difference (that is, time lag). To avoid any explicit reference to the *shape* of mesh stiffness variation, this work deals with the mesh tooth variation functions $k_{sn}(t), k_{rn}(t)$ representing the number of teeth in contact. Attention is focused solely on the relative phase differences of the mesh tooth variations, and these relative phase differences are exactly the same as for the mesh stiffness variation functions.

The mesh phasing quantities under consideration are (Figure 2): 1) γ_{sn} = relative phase between the *n*th sun-planet mesh and the arbitrarily chosen first sun-planet mesh ($\gamma_{s1} = 0$ without loss of generality), 2) γ_{rn} = relative phase between the *n*th ring-planet mesh and the first ring-planet mesh, and 3) $\gamma_{rs}^{(n)}$ = relative phase between the ring-planet *n* mesh and sun-planet *n* mesh. We show subsequently that $\gamma_{rs}^{(n)}$ is independent of the planet under consideration and no superscript is required. The phasings γ_{sn}, γ_{rn}, and $\gamma_{rs}^{(n)}$ are most naturally referenced to the pitch points of the ring-planet and sun-planet meshes, although they can be referenced to any arbitrary point within the mesh such as a change in the number of teeth in contact (Figure 2). All phasings are expressed as a fraction of the mesh period T_m, where T_m is the same for the sun-planet and ring-planet meshes. The convention here is to retain only the fractional (decimal) portion of γ_{sn}, γ_{rn}, and $\gamma_{rs}^{(n)}$, ignoring the whole number portion that represents an integer number of mesh cycles of phase difference. We admit the range $-1 < \gamma_{sn}, \gamma_{rn}, \gamma_{rs}^{(n)} < 1$, but one could restrict these further to $0 \le \gamma_{sn}, \gamma_{rn}, \gamma_{rs}^{(n)} < 1$.

The mesh phasing relationships differ slightly depending on the direction of planet rotation, which is dictated by which element (sun, carrier, or ring) is fixed, which is the input element, and what the input element rotation direction is. There are twelve possible combinations as listed in 1. The mesh phasing relations are defined by the following equations:

Clockwise Planet Rotation

$$\gamma_{sn} = \frac{Z_s \psi_n}{2\pi} \qquad \gamma_{rn} = -\frac{Z_r \psi_n}{2\pi} \tag{1}$$

Counter-clockwise Planet Rotation

$$\gamma_{sn} = -\frac{Z_s \psi_n}{2\pi} \qquad \gamma_{rn} = \frac{Z_r \psi_n}{2\pi} \tag{2}$$

where $Z_{r,s}$ = ring and sun tooth numbers, and ψ_n = circumferential angle of planets measured positive counter-clockwise (Figure 1, $\psi_1 = 0$). The signs of γ_{sn}, γ_{rn} are important to dictate phase lag (plus sign) or phase lead (minus sign) as shown in Figure 2. With the exception of the plus/minus signs, the relations in (1) and (2) can be determined intuitively. For example, consider γ_{rn}. For a fixed ring gear, planet 1 completes Z_r tooth meshes in one complete revolution of the carrier that brings planet 1 back to its initial location. Consequently, when the carrier rotates an angle ψ_n to bring planet 1 to the initial position of planet *n*, $Z_r\psi_n/2\pi$ tooth meshes are completed, giving the expression for γ_{rn}. To determine γ_{sn}, imagine a fixed sun system. Under a complete revolution of the carrier that moves planet 1 through an angle 2π, planet 1 completes Z_s tooth meshes. Accordingly, $Z_s\psi_n/2\pi$ tooth meshes are completed in a partial carrier rotation that moves planet 1 from its initial orientation to the initial orientation of planet *n*. Despite these arguments based on a specific fixed element, (1) and (2) apply for any configuration of fixed and input elements. The relative phase between any two planets numbered i and j are obtained by replacing ψ_n with $\psi_i - \psi_j$ in (1) and (2).

Equations (1) and (2) define the mesh phasing of each planet relative to the first planet for each of the sun meshes and ring meshes individually. They do not define the relative phase $\gamma_{rs}^{(n)}$ between the sun and ring meshes for a given planet (Figure 2). $\gamma_{rs}^{(n)}$ can be any value from -1 to 1 and is not restricted to be 0 or 1/2 depending on the planet having an even or odd number of teeth (as has been previously suggested). $\gamma_{rs}^{(n)}$ does not vary from planet to planet as shown by the following calculation, where $\gamma_{rs}^{(1)}$ is the relative phase between the ring-planet and sun-planet meshes for the first planet,

$$\gamma_{rs}^{(n)} = (\gamma_{rn} + \gamma_{rs}^{(1)}) - \gamma_{sn} = \left(-\frac{Z_r\psi_n}{2\pi} + \gamma_{rs}^{(1)}\right) - \frac{Z_s\psi_n}{2\pi} = \left(\gamma_{rs}^{(1)} - (Z_r + Z_s)\frac{\psi_n}{2\pi}\right) \tag{3}$$

To assemble a planetary gear, the circumferential orientation of each of the planets (ψ_n) must be an integer multiple of the least mesh angle, so

$$\psi_n = p_n \frac{2\pi}{Z_r + Z_s} \tag{4}$$

where p_n is an integer that varies for each planet. Substitution of (4) into (3) yields

$$\gamma_{rs}^{(n)} = \gamma_{rs}^{(1)} - p_n \tag{5}$$

Because p_n is an integer and mesh phase is unaffected by addition or subtraction of an integer number of mesh cycles, we conclude that $\gamma_{rs}^{(n)} = \gamma_{rs}^{(1)}$. Consequently, the relative phase between the ring-planet mesh and sun-planet mesh at a given planet is the same as for all other planets, and the superscript is not necessary ($\gamma_{rs}^{(n)} = \gamma_{rs}$). This result does not depend on equal planet spacing. Calculation of γ_{rs} is discussed subsequently. An equivalent calculation for counter-clockwise planet rotation yields identical conclusions.

The *n*th ring-planet mesh phase relative to the first sun-planet mesh (which we specified to have zero phase at its pitch point) is calculable as either

$$\hat{\gamma}_{rn} = \gamma_{rs} + \gamma_{rn} = \gamma_{sn} + \gamma_{rs} \tag{6}$$

The first equality is the phase between the ring-planet 1 mesh and the sun-planet 1 mesh plus the phase of the ring-planet *n* mesh relative to the ring-planet 1 mesh. The second equality is the phase between the *n*th sun-planet mesh and the first sun-planet mesh plus the phase between the *n*th ring-planet mesh and the *n*th sun-planet mesh.

Equation (6) suggests that $\gamma_{rn} = \gamma_{sn}$, and this is indeed the case. Substitution of (4) into (1) yields the alternate forms of phasing relationships for clockwise planet rotation

$$\gamma_{sn} = \frac{Z_s p_n}{Z_s + Z_r} \qquad \gamma_{rn} = -\frac{Z_r p_n}{Z_s + Z_r} \tag{7}$$

The following calculation shows $\gamma_{rn} = \gamma_{sn}$

$$\gamma_{rn} = -\frac{Z_r p_n}{Z_s + Z_r} = p_n\left[-\frac{Z_r}{Z_s + Z_r} + \frac{Z_s + Z_r}{Z_s + Z_r}\right] = \frac{Z_s p_n}{Z_s + Z_r} = \gamma_{sn} \tag{8}$$

where the second equality invokes the fact that addition of an integer number of complete mesh cycles does not affect the phase. Similar results follow from (2).

The mesh tooth variation functions obey

$$\begin{aligned} k_{sn}(t) &= k_{s1}(t - \gamma_{sn} T_m) \\ k_{rn}(t) &= k_{r1}(t - \gamma_{rn} T_m) \end{aligned} \tag{9}$$

where all $k_{sn}(t)$ and $k_{rn}(t)$ are periodic at the mesh period T_m. Without loss of generality, we choose $t = 0$ to correspond to the point at which the sun-planet 1 mesh is at the pitch point. Periodicity of k_{s1} ensures it has a Fourier series representation; with (9) this yields

$$\begin{aligned} k_{s1}(t) &= \sum_{l=0}^{\infty} [a_l \sin l\omega_m t + b_l \cos l\omega_m t] \\ k_{sn}(t) &= \sum_{l=0}^{\infty} [a_l \sin l\omega_m (t - \gamma_{sn} T_m) + b_l \cos l\omega_m (t - \gamma_{sn} T_m)] \end{aligned} \tag{10}$$

For the ring-planet meshes,

$$\begin{aligned} k_{r1}(t) &= \sum_{l=0}^{\infty} [c_l \sin l\omega_m (t) + d_l \cos l\omega_m (t)] \\ k_{rn}(t) &= \sum_{l=0}^{\infty} [c_l \sin l\omega_m (t - \gamma_{rn} T_m) + d_l \cos l\omega_m (t - \gamma_{rn} T_m)] \end{aligned} \tag{11}$$

Expressions of the form (10)-(11) can be used to analytically derive results for suppression of vibration in planetary gears [2, 3].

The phase shift γ_{rs} between the ring-planet mesh and sun-planet mesh is implicit in (9) because the k_{rn} are defined in terms of k_{r1}. Note that $t = 0$ in k_{r1} corresponds to the *sun*-planet 1 (*not* ring-planet 1) pitch point (and the Fourier series in (11) must be calculated accordingly). Letting $M_{r1}(\tau)$ be the mesh tooth variation function of the ring-planet 1 mesh with $\tau = 0$ being the pitch point of the *ring*-planet 1 mesh (as might be generated by gear analysis software), then

$$\begin{aligned} k_{r1}(t) &= M_{r1}(t - \gamma_{rs} T_m) \\ k_{rn}(t) &= M_{r1}(t - (\gamma_{rs} + \gamma_{rn}) T_m) = M_{r1}(t - \hat{\gamma}_{rn} T_m) \end{aligned} \tag{12}$$

The results of this section apply for helical and spur planetary gears. Because the results depend only on the tooth numbers and planet circumferential orientations ψ_n, the results also apply to modified gear teeth. Tooth modifications may change the shape of the mesh tooth variation (and mesh stiffness variation) functions, but they do not change the phasing.

Analytical Calculation of k_{sn}, k_{rn}, and γ_{rs}

The mesh tooth variation functions shown in Figure 2 can be calculated analytically based on gear design parameters. Considering unmodified, involute spur gears, the following discussion refers to Figure 3, where a representative mesh tooth variation function is shown in Figure 3a with the highlighted points defined as: **B**, point where second tooth enters contact; **C**, point where first tooth exits contact; **P**, second tooth at pitch

point; **D**, point where third tooth enters contact; and **E**, point where second tooth exits contact. By virtue of the phasing relations (1) and (2), the functions k_{sn}, k_{rn} are fully defined for *all* meshes provided one can find them for the arbitrarily chosen first planet. It is sufficient to calculate the lengths **BE**, **BC**, **BP**, and **BD** in Figure 3a. The calculations follow from the geometry of Figure 3b.

For the sun-planet mesh

$$\begin{aligned}\mathbf{B}_1\mathbf{E}_1 &= \mathbf{M}_1\mathbf{E}_1 + \mathbf{B}_1\mathbf{N}_1 - \mathbf{M}_1\mathbf{N}_1 \\ &= \sqrt{R_{so}^2 - R_{sb}^2} + \sqrt{R_{po}^2 - R_{pb}^2} - (R_{sb} + R_{pb})\tan\alpha_1\end{aligned} \tag{13}$$

where the notation is defined in the caption of Figure 3. Also,

$$\mathbf{B}_1\mathbf{P}_1 = \mathbf{M}_1\mathbf{P}_1 - \mathbf{M}_1\mathbf{B}_1 = R_{sb}\tan\alpha_1 - \left(\sqrt{R_{so}^2 - R_{sb}^2} - \mathbf{B}_1\mathbf{E}_1\right) \tag{14}$$

The base pitch is $p = 2\pi R_{sb}/Z_s = 2\pi R_{pb}/Z_p$, and

$$\mathbf{B}_1\mathbf{C}_1 = \mathbf{B}_1\mathbf{E}_1 - p \qquad \mathbf{B}_1\mathbf{D}_1 = p \tag{15}$$

For the ring-planet mesh,

$$\begin{aligned}\mathbf{B}_2\mathbf{E}_2 &= \mathbf{M}_2\mathbf{N}_2 + \mathbf{N}_2\mathbf{E}_2 - \mathbf{M}_2\mathbf{B}_2 \\ &= \mathbf{O}_1\mathbf{O}_2\sin\alpha_2 + \sqrt{R_{po}^2 - R_{pb}^2} - \sqrt{R_{ro}^2 - R_{rb}^2}\end{aligned} \tag{16}$$

$$\mathbf{B}_2\mathbf{P}_2 = \mathbf{M}_2\mathbf{P}_2 - \mathbf{M}_2\mathbf{B}_2 = R_{rb}\tan\alpha_2 - \sqrt{R_{ro}^2 - R_{rb}^2} \tag{17}$$

$$\mathbf{B}_2\mathbf{C}_2 = \mathbf{B}_2\mathbf{E}_2 - p \qquad \mathbf{B}_2\mathbf{D}_2 = p \tag{18}$$

where $\mathbf{O}_1\mathbf{O}_2 = (R_{sb} + R_{pb})/\cos\alpha_1$ and the base pitch p is unchanged.

The shapes of k_{s1}, k_{r1} are fully defined by (13)-(18). With $t = 0$ corresponding to the pitch point of k_{s1}, all k_{sn} are determined by (1), (2), and (9). The k_{rn} defined in (12) require γ_{rs}. γ_{rs} is determined from the points $\mathbf{Q}_{1,\,2,\,3}$ on Figure 3b. These points locate the pitch point of the ring-planet mesh relative to the pitch point of the sun-planet mesh. $\mathbf{Q}_1$ is the image of $\mathbf{P}_1$ when the contact line $\mathbf{M}_1\mathbf{N}_1$ is wrapped on the planet base circle. Because ring-planet contact occurs on the opposite planet tooth face than sun-planet mesh, we need $\mathbf{Q}_2$, which is an arclength t_b away from $\mathbf{Q}_1$, where t_b is the planet tooth thickness at the base circle. To determine at what phase the ring-planet mesh is when the sun-planet mesh is at its pitch point, we find the first point in the ring-planet contact region $\mathbf{B}_2\mathbf{E}_2$ that is an integer number of base pitches away from $\mathbf{Q}_2$. That point is denoted $\mathbf{Q}_3$. To find $\mathbf{Q}_3$, we need the length

$$\begin{aligned}\mathbf{Q}_2\mathbf{B}_2 &= \mathbf{P}_1\mathbf{P}_2 - \mathbf{B}_2\mathbf{P}_2 - t_b \\ &= [R_{pb}\tan\alpha_1 + R_{pb}(\pi - \alpha_1 - \alpha_2) + R_{pb}\tan\alpha_2] - \mathbf{B}_2\mathbf{P}_2 - t_b\end{aligned} \tag{19}$$

where $\mathbf{B}_2\mathbf{P}_2$ is given in (17). The position of $\mathbf{Q}_3$ within the contact region $\mathbf{B}_2\mathbf{E}_2$ is

$$\mathbf{B}_2\mathbf{Q}_3 = p[1 - dec(\mathbf{Q}_2\mathbf{B}_2/p)] \tag{20}$$

where $dec(\mathbf{Q}_2\mathbf{B}_2/p)$ is the decimal portion of $\mathbf{Q}_2\mathbf{B}_2/p$. Then, $\mathbf{P}_2\mathbf{Q}_3 = \left|\mathbf{B}_2\mathbf{Q}_3 - \mathbf{B}_2\mathbf{P}_2\right|$. When the first sun-planet mesh is at the pitch point, the first ring-planet mesh is at position $\mathbf{Q}_3$. Consequently, the *magnitude* of the relative phase between the pitch points is

$$\left|\gamma_{rs}\right| = (\mathbf{P}_2\mathbf{Q}_3)/p \tag{21}$$

The magnitude of γ_{rs} is independent of which element is fixed, which is the input, or the direction of rotation.

The sign of γ_{rs} must be established, and this depends on: 1) whether $\mathbf{Q}_3$ falls within $\mathbf{B}_2\mathbf{P}_2$ or $\mathbf{P}_2\mathbf{E}_2$, and 2) whether contact along the line of action progresses from $\mathbf{B} \to \mathbf{E}$ or $\mathbf{E} \to \mathbf{B}$ (both the sun-planet and ring-planet meshes progress in the same direction for all possible planetary (epicyclic) gear configurations). The direction of contact along the line of action is indicated in 1 for all configurations. As ring-planet contact progresses along $\mathbf{B} \to \mathbf{E}$ (or $\mathbf{E} \to \mathbf{B}$, as appropriate for the configuration (1)) $\gamma_{rs} = -\left|\gamma_{rs}\right| < 0$ if contact condition $\mathbf{Q}_3$ occurs after pitch point contact $\mathbf{P}_2$, and $\gamma_{rs} = \left|\gamma_{rs}\right| > 0$ if contact condition $\mathbf{Q}_3$ occurs before pitch point contact $\mathbf{P}_2$ (2).

While equations (13)-(18) hold only for unmodified spur gears, (21) depends only on the relative positions of the pitch points and holds for modified spur gears.

Example

The example results in Figures 4 and 5 come from analysis of the US Army OH58 Kiowa helicopter planetary as described in [10] (3). For these parameters (1) or (7) yield the following for clockwise planet rotation, where the arrows indicate removal of the integer portion such that $-1 < \gamma_{sn}, \gamma_{rn} < 1$

$$\begin{Bmatrix}\gamma_{s1}\\ \gamma_{s2}\\ \gamma_{s3}\\ \gamma_{s4}\end{Bmatrix} = \frac{27}{2\pi}\begin{Bmatrix}0\\ \frac{32\pi}{63}\\ \pi\\ \frac{95\pi}{63}\end{Bmatrix} = \begin{Bmatrix}0\\ 48/7\\ 27/2\\ 285/14\end{Bmatrix} \rightarrow \begin{Bmatrix}0\\ 6/7\\ 1/2\\ 5/14\end{Bmatrix}$$

$$\begin{Bmatrix}\gamma_{r1}\\ \gamma_{r2}\\ \gamma_{r3}\\ \gamma_{r4}\end{Bmatrix} = -\frac{99}{2\pi}\begin{Bmatrix}0\\ \frac{32\pi}{63}\\ \pi\\ \frac{95\pi}{63}\end{Bmatrix} = \begin{Bmatrix}0\\ -176/7\\ -99/2\\ -1045/14\end{Bmatrix} \rightarrow \begin{Bmatrix}0\\ -1/7\\ -1/2\\ -9/14\end{Bmatrix} \quad (22)$$

For this system, the number of teeth in contact at each mesh was determined over two mesh cycles using a contact calculation based on precise involute tooth geometry at no load. The results shown in Figure 4 for fixed ring and counter-clockwise carrier input confirm the analytical predictions in (22). Notice that the negative signs in γ_{rn} correspond to phase lead as expected from (9). All six clockwise planet rotation cases (1) were calculated and yielded identical phasing γ_{sn} and γ_{rn}. The sign of γ_{rs} can differ between these six cases, however, as shown in 1 and 2. The steps leading to $|\gamma_{rs}|$ in (21) give $\mathbf{B}_2\mathbf{P}_2 = 4.981\ mm$, $\mathbf{B}_2\mathbf{Q}_3 = 5.250\ mm$, and $|\gamma_{rs}| = 0.0329$. With $\mathbf{B}_2\mathbf{Q}_3 > \mathbf{B}_2\mathbf{P}_2$, the contact progression at the ring-planet mesh for fixed ring and carrier input is $\mathbf{E}_2 \rightarrow \mathbf{Q}_3 \rightarrow \mathbf{P}_2 \rightarrow \mathbf{B}_2$. Consequently, $\gamma_{rs} = 0.0329 > 0$ from 2, which is consistent with the numerical contact solution of Figure 4.

For counter-clockwise planet rotation, (2) yields mesh phasing opposite in sign to (22)

$$\begin{Bmatrix}\gamma_{s1}\\ \gamma_{s2}\\ \gamma_{s3}\\ \gamma_{s4}\end{Bmatrix} = -\frac{27}{2\pi}\begin{Bmatrix}0\\ \frac{32\pi}{63}\\ \pi\\ \frac{95\pi}{63}\end{Bmatrix} \rightarrow \begin{Bmatrix}0\\ -6/7\\ -1/2\\ -5/14\end{Bmatrix}$$

$$\begin{Bmatrix}\gamma_{r1}\\ \gamma_{r2}\\ \gamma_{r3}\\ \gamma_{r4}\end{Bmatrix} = \frac{99}{2\pi}\begin{Bmatrix}0\\ \frac{32\pi}{63}\\ \pi\\ \frac{95\pi}{63}\end{Bmatrix} \rightarrow \begin{Bmatrix}0\\ 1/7\\ 1/2\\ 9/14\end{Bmatrix} \quad (23)$$

The corresponding numerical results from no-load involute contact analysis of the fixed ring, clockwise sun input case are shown in Figure 5 and agree with (23). All counter-clockwise planet rotation conditions (1) were confirmed by numerical contact solution to yield phasing γ_{sn} and γ_{rn} identical to (23). Because $\gamma_{s2}, \gamma_{s3}, \gamma_{s4} < 0$, the sun meshes lead the sun-planet 1 mesh (see (9)). The magnitude of γ_{rs} is the same as above. For the fixed ring, sun input case, the contact progression is $\mathbf{B}_2 \rightarrow \mathbf{P}_2 \rightarrow \mathbf{Q}_3 \rightarrow \mathbf{E}_2$ (1), giving $\gamma_{rs} = -0.0329 < 0$ from 2. This result is confirmed in Figure 5.

In both example cases, (13)-(18) are all satisfied in the numerically calculated mesh tooth variation results. Also, $\gamma_{rs}^{(n)} = \gamma_{rs}$ is the same for all planets.

Acknowledgments

The authors thank Mr. Vijaya Kumar Ambarisha and Mr. Gang Liu for their help in validating the analytical phasing results. This material is based upon work supported by the U.S. Army Research Office under grant DAAD19-99-1-0218.

References

1.Schlegel, R.G. and K.C. Mard. *Transmission Noise Control Approaches in Helicopter Design*. in *ASME Design Engineering Conference*. 1967. New York: ASME paper 67-DE-58.

2.Seager, D.L., *Conditions for the Neutralization of Excitation by the Teeth in Epicyclic Gearing*. Journal of Mechanical Engineering Science, 1975. **17**(5): p. 293-298.

3.Parker, R.G., *A Physical Explanation for the Effectiveness of Planet Phasing to Suppress Planetary Gear Vibration*. Journal of Sound and Vibration, 2000. **236**(4): p. 561-573.

4.Kahraman, A. and G.W. Blankenship. *Planet Mesh Phasing in Epicyclic Gearsets*. in *International Gearing Conference*. 1994. Newcastle, UK.

5.Lin, J. and R.G. Parker, *Parametric Instability in Planetary Gears under Mesh Stiffness Variation*. Journal of Sound and Vibration, 2002. **249**(1): p. 129-145.

6.Kahraman, A., *Planetary Gear Train Dynamics*. Journal of Mechanical Design, 1994. **116**: p. 713-720.

7.Kahraman, A., *Load Sharing Characteristics of Planetary Transmissions*. Mechanism and Machine Theory, 1994. **29**: p. 1151-1165.

8.August, R. and R. Kasuba, *Torsional Vibrations and Dynamic Loads in a Basic Planetary Gear System*. Journal of Vibration, Acoustics, Stress and Reliability in Design, 1986. **108**(3): p. 348-353.

9.Velex, P. and L. Flamand, *Dynamic Response of Planetary Trains to Mesh Parametric Excitations*. Journal of Mechanical Design, 1996. **118**: p. 7-14.

10.Parker, R.G., V. Agashe, and S.M. Vijayakar, *Dynamic Response of a Planetary Gear System Using a Finite Element/Contact Mechanics Model*. ASME Journal of Mechanical Design, 2000. **122**(3): p. 304-310.

11.Lin, J. and R.G. Parker, *Analytical Characterization of the Unique Properties of Planetary Gear Free Vibration*. Journal of Vibration and Acoustics, 1999. **121**: p. 316-321.

12.Parker, R.G. and J. Lin, *Mesh Phasing Relationships in Planetary and Epicyclic Gears*. ASME Journal of Mechanical Design, 2003. **submitted**.

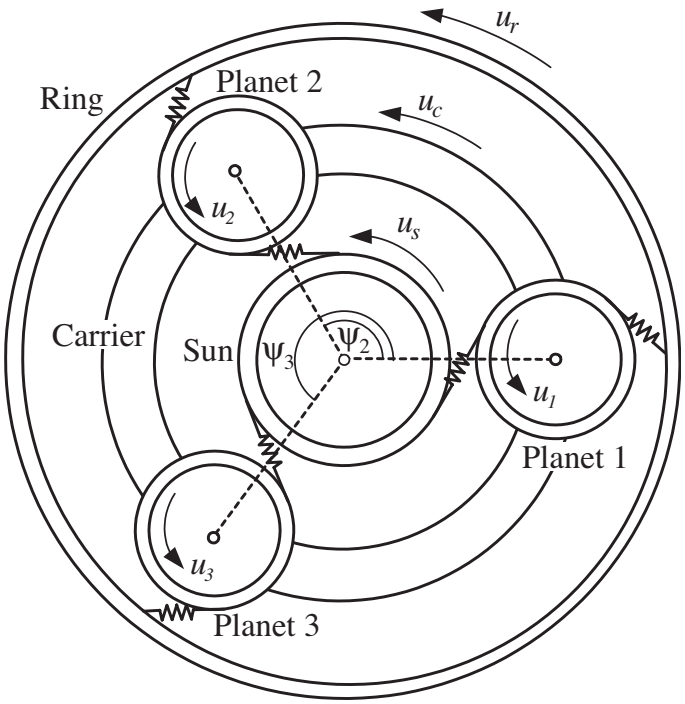

Figure 1: Planetary (or epicyclic) gear system.

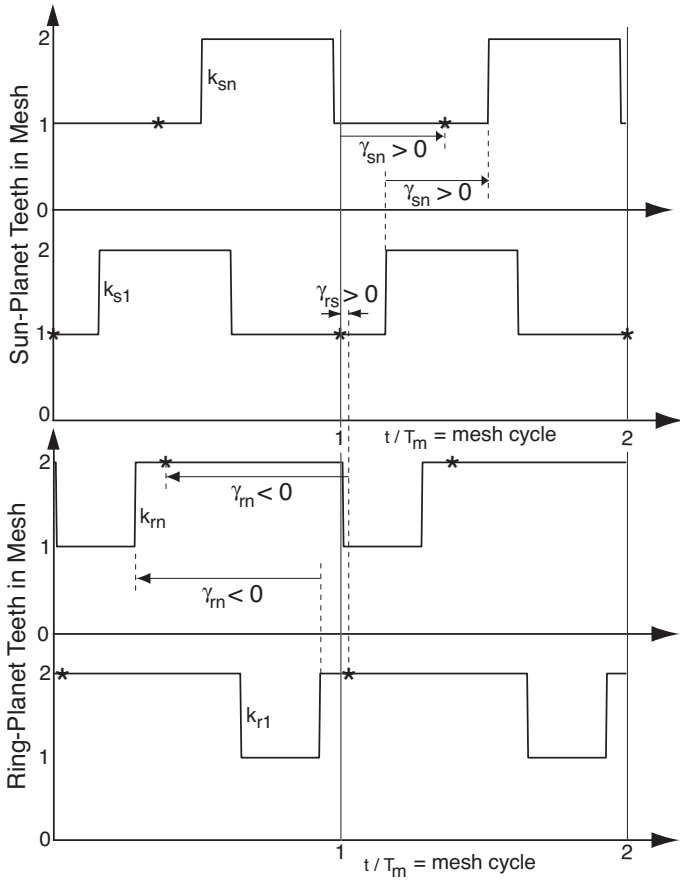

Figure 2: Definition of mesh phase quantities γ_{sn}, γ_{rn}, γ_{rs}. Without loss of generality, $\gamma_{s1} = 0$, and $t = 0$ corresponds to pitch point contact at the sun-planet 1 mesh. The * denotes pitch point contact.

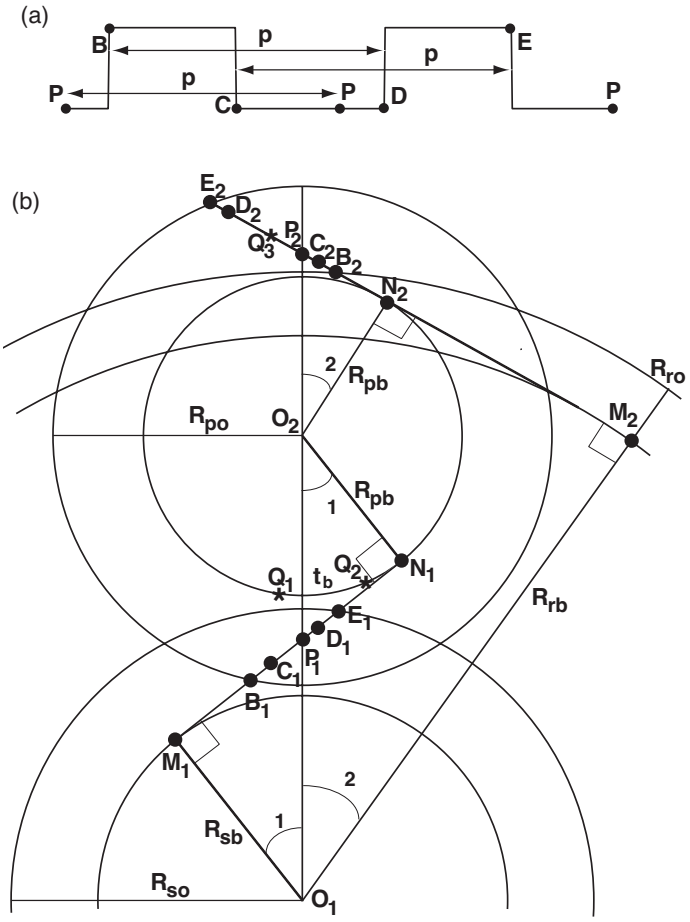

Figure 3: (a) Example mesh tooth variation functions showing the number of teeth in contact. **P** is the pitch point. **p** denotes the base pitch. (b) Sun-planet and ring-planet mesh details. R_{sb}, R_{pb}, R_{rb} denotes base radii. R_{so}, R_{po} indicate sun and planet outer radii; R_{ro} is the inner radius of the ring gear teeth. $\alpha_{1,2}$ are pressure angles. The points **B**, **C**, **P**, **D**, and **E** at each of the two meshes correspond to the points indicated in (a).

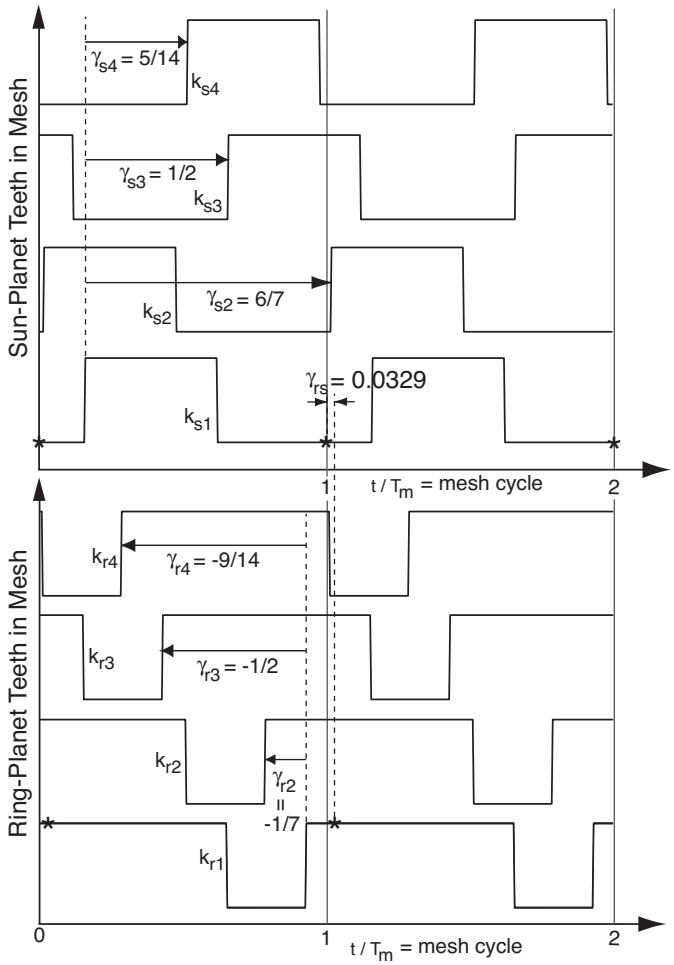

Figure 4: Mesh tooth variations at each of the sun-planet and ring-planet meshes for the example system with fixed ring and counter-clockwise carrier input (clockwise planet rotation) as derived using finite element/contact mechanics software for involute teeth at no load. Each curve fluctuates between one and two. The symbol * denotes pitch point contact. The results agree with (1), (21), and the sign of $\gamma_{rs} > 0$ as dictated by 1 and 2.

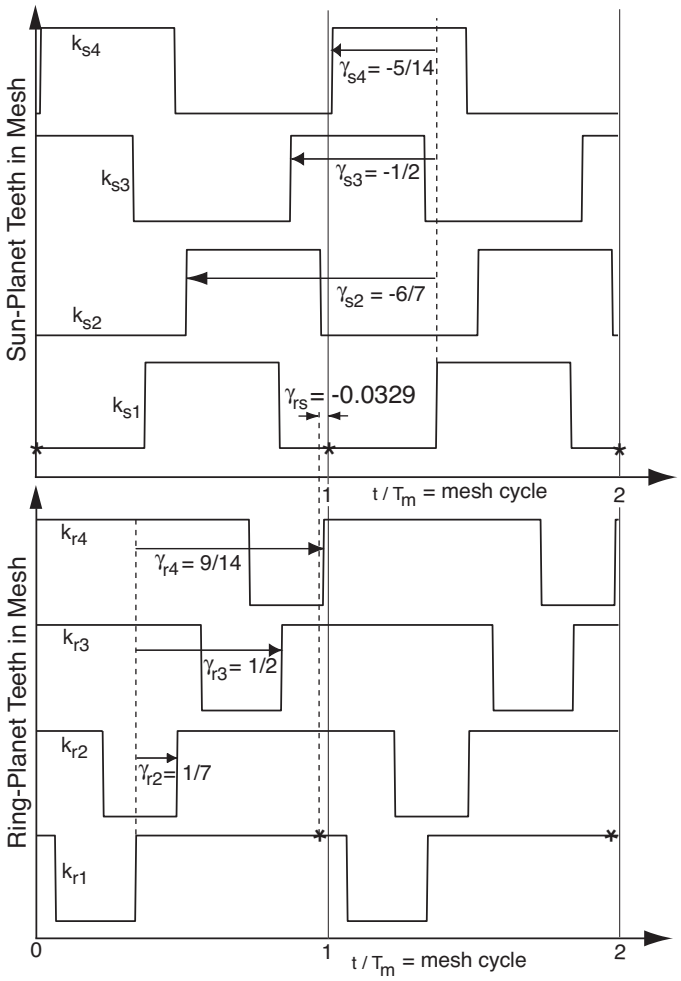

Figure 5: Mesh tooth variations at each of the sun-planet and ring-planet meshes for the example system with fixed ring and clockwise sun input (counter-clockwise planet rotation) as derived using finite element/contact mechanics software for involute teeth at no load. Each curve fluctuates between one and two. The symbol * denotes pitch point contact. The results agree with (2), (21), and the sign of $\gamma_{rs} < 0$ as dictated by 1 and 2.

				Contact Progression on Line of Action (see Figure 3b)	
Fixed	**Input**	**Input Rotation**	**Planet Rotation**	**Sun-Planet Mesh**	**Ring-Planet Mesh**
Ring	Sun	CW	CCW	$\mathbf{B}_1 \rightarrow \mathbf{E}_1$	$\mathbf{B}_2 \rightarrow \mathbf{E}_2$
	Sun	CCW	CW	$\mathbf{B}_1 \rightarrow \mathbf{E}_1$	$\mathbf{B}_2 \rightarrow \mathbf{E}_2$
	Carrier	CW	CCW	$\mathbf{E}_1 \rightarrow \mathbf{B}_1$	$\mathbf{E}_2 \rightarrow \mathbf{B}_2$
	Carrier	CCW	CW	$\mathbf{E}_1 \rightarrow \mathbf{B}_1$	$\mathbf{E}_2 \rightarrow \mathbf{B}_2$
Sun	Carrier	CW	CW	$\mathbf{B}_1 \rightarrow \mathbf{E}_1$	$\mathbf{B}_2 \rightarrow \mathbf{E}_2$
	Carrier	CCW	CCW	$\mathbf{B}_1 \rightarrow \mathbf{E}_1$	$\mathbf{B}_2 \rightarrow \mathbf{E}_2$
	Ring	CW	CW	$\mathbf{E}_1 \rightarrow \mathbf{B}_1$	$\mathbf{E}_2 \rightarrow \mathbf{B}_2$
	Ring	CCW	CCW	$\mathbf{E}_1 \rightarrow \mathbf{B}_1$	$\mathbf{E}_2 \rightarrow \mathbf{B}_2$
Carrier	Sun	CW	CCW	$\mathbf{B}_1 \rightarrow \mathbf{E}_1$	$\mathbf{B}_2 \rightarrow \mathbf{E}_2$
	Sun	CCW	CW	$\mathbf{B}_1 \rightarrow \mathbf{E}_1$	$\mathbf{B}_2 \rightarrow \mathbf{E}_2$
	Ring	CW	CW	$\mathbf{E}_1 \rightarrow \mathbf{B}_1$	$\mathbf{E}_2 \rightarrow \mathbf{B}_2$
	Ring	CCW	CCW	$\mathbf{E}_1 \rightarrow \mathbf{B}_1$	$\mathbf{E}_2 \rightarrow \mathbf{B}_2$

Table 1: Categorization of possible fixed element, input element, and input rotation direction combinations into: a) direction of planet rotation, and b) two possible directions of mesh progression along the lines of action. $\mathbf{B}_1$, $\mathbf{E}_1$, $\mathbf{B}_2$, $\mathbf{E}_2$ refer to points in Figure 3b. CCW denotes counter-clockwise and CW denotes clockwise.

Sun/Ring-Planet Contact Progression	$\gamma_{rs} > 0$	$\gamma_{rs} < 0$
$\mathbf{B} \rightarrow \mathbf{E}$	$\mathbf{B}_2 \rightarrow \mathbf{Q}_3 \rightarrow \mathbf{P}_2 \rightarrow \mathbf{E}_2$	$\mathbf{B}_2 \rightarrow \mathbf{P}_2 \rightarrow \mathbf{Q}_3 \rightarrow \mathbf{E}_2$
$\mathbf{E} \rightarrow \mathbf{B}$	$\mathbf{E}_2 \rightarrow \mathbf{Q}_3 \rightarrow \mathbf{P}_2 \rightarrow \mathbf{B}_2$	$\mathbf{E}_2 \rightarrow \mathbf{P}_2 \rightarrow \mathbf{Q}_3 \rightarrow \mathbf{B}_2$

Table 2: Contact progressions at the ring-planet mesh for $\gamma_{rs} < 0$ and $\gamma_{rs} > 0$. The sign of γ_{rs} is governed by whether $\mathbf{Q}_3$ occurs before or after the pitch point $\mathbf{P}_2$. The contact progression $\mathbf{B} \rightarrow \mathbf{E}$ or $\mathbf{E} \rightarrow \mathbf{B}$ at the sun/ring-planet meshes is dictated by the configuration and direction of rotation as shown in 1.

	Sun	Planet	Ring
Teeth	27	35	99
Base Radius (*mm*)	35.19	45.63	129.1
Major Radius (Minor for ring) (*mm*)	42.02	52.44	135.9
Sun-planet pressure angle, $\alpha_1 = 24.6034$ ***deg***			
Ring-planet pressure angle, $\alpha_2 = 20.1915$ ***deg***			
Planet tooth thickness at base circle, $t_b = 6.365$ ***mm***			
Planet spacing (*rad*): $\psi_1 = 0, \psi_2 = 32\pi/63, \psi_3 = \pi, \psi_4 = 95\pi/63$ $\Rightarrow \quad p_1 = 0, p_2 = 32, p_3 = 63, p_4 = 95$			

Table 3: Gear parameters for example system.